

---

# Endowing Interpretability for Neural Cognitive Diagnosis by Efficient Kolmogorov-Arnold Networks

---

Shangshang Yang<sup>1</sup>

Linrui Qin<sup>2</sup>

Xiaoshan Yu<sup>1</sup>

<sup>1</sup>School of Artificial Intelligence, Anhui University,

<sup>2</sup>School of Computer Science and Technology, Anhui University  
Hefei 230601, China

{yangshang0308, stonewallqr, yxsleo}@gmail.com

## Abstract

In the realm of intelligent education, cognitive diagnosis plays a crucial role in subsequent recommendation tasks attributed to the revealed students' proficiency in knowledge concepts. Although neural network-based neural cognitive diagnosis models (CDMs) have exhibited significantly better performance than traditional models, neural cognitive diagnosis is criticized for the poor model interpretability due to the multi-layer perception (MLP) employed, even with the monotonicity assumption. Therefore, this paper proposes to empower the interpretability of neural cognitive diagnosis models through efficient kolmogorov-arnold networks (KANs), named KAN2CD, where KANs are designed to enhance interpretability in two manners. Specifically, in the first manner, KANs are directly used to replace the used MLPs in existing neural CDMs; while in the second manner, the student embedding, exercise embedding, and concept embedding are directly processed by several KANs, and then their outputs are further combined and learned in a unified KAN to get final predictions. To overcome the problem of training KANs slowly, we modify the implementation of original KANs to accelerate the training. Experiments on four real-world datasets show that the proposed KA2NCD exhibits better performance than traditional CDMs, and the proposed KA2NCD still has a bit of performance leading even over the existing neural CDMs. More importantly, the learned structures of KANs enable the proposed KA2NCD to hold as good interpretability as traditional CDMs, which is superior to existing neural CDMs. Besides, the training cost of the proposed KA2NCD is competitive to existing models.

## 1 Introduction

As a crucial technique in intelligent education, cognitive diagnosis (CD) [2, 5] is responsible for revealing students' proficiency in knowledge concepts by mining their historical records of answering exercises. For better understanding, an illustrative example of the CD process is given in Fig. 1. In this case, two students' response records are given ((i.e.,  $\{e_1, e_3, e_4\}$  and  $\{e_1, e_2, e_3\}$ )) and the relationships between exercises and knowledge concepts are also depicted through an exercise-concept relational matrix ( $Q$ -matrix for short). As can be

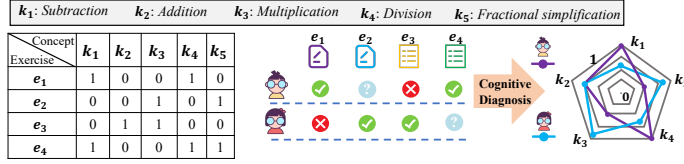


Figure 1: Illustration of cognitive diagnosis process of two students.

seen, the CD process models the student answering prediction to obtain the two students' knowledge mastery states by mining their response records and utilizing the  $Q$ -matrix. With the diagnosed students' knowledge proficiency, many subsequent tasks [30, 3] on online education platforms can provide more accurate and higher quality services, such as remedial instruction, learning path recommendations, targeted training, and exercise/course assembly.

To develop convincing cognitive diagnosis models (CDMs) for meeting the demands of fast-growing education platforms (e.g., ASSISTments [23], PTA [14]), massive efforts have been devoted by researchers in different domains, mainly from two research perspectives. The first perspective is to design completely interpretable CDMs whose components and operations are drawn from educational psychology, so that the users (including students, teachers, and parents) are able to understand how the diagnosis results are obtained, trusting the results. The representatives include IRT [10], DINA [26], MIRT [24], and MF [18]. The second perspective is to leverage neural networks (NNs) to model the student's response prediction process, aiming to improve the prediction accuracy and provide more accurate diagnosis results for making subsequent tasks like recommendations more convincing. This type of CDMs is called neural cognitive diagnosis models due to the NNs used, and the representatives contain NCD [28], KaNCD [29], (RCD) [13], and so on [21].

Compared to traditional CDMs in educational psychology, neural CDMs indeed exhibit significantly better performance [28], which can make subsequent tasks benefit more. Despite that, the model interpretability of neural CDMs is not as good as that of traditional CDMs because these models more or less employ the multi-layer perceptions (MLPs), i.e., multiple fully connected (FC) layers [11]. It is difficult to interpret what roles the employed MLPs or FC layers play and how they process the inputs to get the output prediction [31] even equipped with the monotonicity assumption [25]. This monotonicity property can only ensure that their weights are positive and their outputs are monotonically increasing with the inputs [28], which can not make users understand how the diagnosis results are obtained. As a result, neural CDMs' limited interpretability hampers their ability to engage users convincingly to some extent.

To this end, this paper aims to build more convincing CDMs by enhancing the interpretability of neural cognitive diagnosis models without sacrificing the accuracy of the diagnosis results. Thus, this paper proposes leveraging efficient Kolmogorov-Arnold networks for neural cognitive diagnosis models (KA2NCD) to empower the model's interpretability and maintain the accuracy of diagnosis. Specifically, our main contributions are as follows:

- This paper is the first work to leverage Kolmogorov-Arnold networks (KANs) to empower the interpretability of neural CDMs while maintaining high diagnosis accuracy. To achieve this, we propose two manners of using KANs for neural CD. The first is replacing MLPs in neural CDMs by KANs to enhance their interpretability directly, and the second is designing a completely new aggregation framework consisting of multiple KANs without the help of any neural CDMs.
- In the new aggregation framework, there exist two levels of KANs to handle input and output the prediction. Several KANs at the lower level are used to directly process the student embedding, exercise embedding, and concept embedding, respectively. Then, a unified two-layer KAN at the upper level is used to further combine and learn the outputs of lower-level KANs to get final predictions. Besides, considering high runtime in the original implementation of KANs, we modified the implementation of KANs to accelerate the training.

- To validate the effectiveness of the proposed KA2NCD, we compare it with some representative CDMs on four popular education datasets. Experimental results show that the proposed KA2NCD achieves better performance than traditional CDMs and neural CDMs. Besides, the learned structures of KANs in the proposed KA2NCD also demonstrate its higher interpretability than neural CDMs, as good as traditional CDMs. Moreover, the modified implementation of KANs makes the training cost of the proposed KA2NCD competitive to existing models.

## 2 Preliminaries and Related Work

### 2.1 Preliminaries of Cognitive Diagnosis Task

In the cognitive diagnosis task of intelligent education scenarios, we consider  $N$  students,  $M$  exercises, and  $K$  knowledge concepts, represented by the sets  $S = \{s_1, s_2, \dots, s_N\}$ ,  $E = \{e_1, e_2, \dots, e_M\}$ , and  $C = \{c_1, c_2, \dots, c_K\}$  respectively. The platform employs an exercise-concept relation matrix provided by domain experts, referred to as the  $Q$ -matrix, denoted by  $Q = (Q_{jk} \in \{0, 1\})^{M \times K}$ . Here,  $Q_{jk} = 1$  implies that exercise  $e_j$  involves knowledge concept  $c_k$ , and  $Q_{jk} = 0$  indicates no relation between them. Additionally, the platform maintains a log of students' responses to exercises, recorded in  $R_{log}$ . This log comprises triplets  $(s_i, e_j, r_{ij})$ , where  $s_i \in S$ ,  $e_j \in E$ , and  $r_{ij} \in \{0, 1\}$ . In this context,  $r_{ij} = 1$  denotes a correct response by student  $s_i$  to exercise  $e_j$ , whereas  $r_{ij} = 0$  denotes an incorrect response.

By utilizing the students' response logs  $R_{log}$  and the  $Q$ -matrix, the cognitive diagnosis task involves mining students' proficiency in knowledge concepts by developing a model,  $\mathcal{F}$ , to predict students' scores on exercises. The model  $\mathcal{F}$  utilizes three types of input features to predict the score of student  $s_i$  on exercise  $e_j$ : the student-related feature vector  $\mathbf{h}_S \in \mathbb{R}^{1 \times D}$ , the exercise-related feature vector  $\mathbf{h}_E \in \mathbb{R}^{1 \times D}$ , and the knowledge concept-related feature vector  $\mathbf{h}_C \in \mathbb{R}^{1 \times K}$ . Specifically, the embedding for students, exercises, and knowledge concepts can be obtained as follows:

$$\begin{aligned} \mathbf{h}_S &= \mathbf{x}_i^S \times W_S, W_S \in \mathbb{R}^{N \times D}, \mathbf{h}_E = \mathbf{x}_j^E \times W_E, W_E \in \mathbb{R}^{M \times D}, \\ \mathbf{h}_C &= \mathbf{x}_j^C \times W_Q, W_Q \in \mathbb{R}^{K \times D}, \mathbf{x}_j^C = \mathbf{x}_j^E \times Q = (Q_{j1}, Q_{j2}, \dots, Q_{jK}), \end{aligned} \quad (1)$$

where  $D$  is the embedding dimension (usually equal to  $K$  for consistency),  $\mathbf{x}_i^S \in \{0, 1\}^{1 \times N}$  is the one-hot vector for student  $s_i$ ,  $\mathbf{x}_j^E \in \{0, 1\}^{1 \times M}$  is the one-hot vector for exercise  $e_j$ , and  $W_S$  and  $W_E$  are trainable matrices in the embedding layers. Then, the model  $\mathcal{F}$  outputs the predicted response  $\hat{r}_{ij}$  as

$$\hat{r}_{ij} = \mathcal{F}(\mathbf{h}_S, \mathbf{h}_E, \mathbf{h}_C), \quad (2)$$

where  $\mathcal{F}(\cdot)$  is the diagnostic function to combine three types of inputs in different manners. Generally speaking, after training the model  $\mathcal{F}$  based on students' response logs, each bit value of  $\mathbf{h}_S$  represents the student's proficiency in the corresponding knowledge concept.

### 2.2 Related Work on Cognitive Diagnosis

In the following, some representatives of traditional CDMs and neural CDMs will be reviewed, which focuses on introducing their prediction process.

#### 2.2.1 Traditional CDMs

As the most typical CDM, DINA [26] outputs the prediction  $\hat{r}_{ij}$  as

$$\hat{r}_{ij} = g^{1-nt}(1-sl)^{nt}, \text{ where } nt = \prod_k \theta_k^{\beta_k}, \beta = \mathbf{h}_C. \quad (3)$$

$\theta \in \{0, 1\}^{1 \times K}$  and  $\beta \in \{0, 1\}^{1 \times K}$  are two binary latent features to indicate which concepts the student mastered and the exercise contains.  $\theta$  can be obtained from  $\mathbf{h}_S$  through a FC layer and Gumbel-Softmax [15]. The guessing factor  $g \in \mathbb{R}^1$  and slipping factor  $sl \in \mathbb{R}^1$  refer to the probability of correctly answering the exercise only with guessing and the probability of mistakenly answering even with the corresponding concept mastered, and

they are transformed from  $\mathbf{h}_E$  by FC layers. As can be seen, the prediction process of DINA is interpretable, but DINA suffers from poor prediction performance on large-scale data.

As another typical CDM, the prediction process of IRT [10] can be denoted as follows:

$$\hat{r}_{ij} = Sigmoid(a(\theta - \beta)), \theta \in \mathbb{R}^1 = FC(\mathbf{h}_S), \beta \in \mathbb{R}^1 = FC(\mathbf{h}_E), a \in \mathbb{R}^1 = FC(\mathbf{h}_E), \quad (4)$$

where  $\theta$  is obtained from  $\mathbf{h}_S$  by an FC layer, denoting the student ability feature.  $\beta$  and  $a$  are transformed from  $\mathbf{h}_E$  by two different FC layers, denoting the exercise difficulty and distinction features. As can be seen, the prediction of IRT can be easily understood and interpreted. However, IRT also does not perform well on some complex datasets.

As a multidimensional variant of IRT, MIRT [24] applies the same logistic function to the linear transformation of the student ability vector  $\boldsymbol{\theta} \in \mathbb{R}^{1 \times K}$ , the exercise difficulty feature  $\beta \in \mathbb{R}^1$ , and the knowledge concept latent vector  $\boldsymbol{\alpha} \in \mathbb{R}^{1 \times K}$ . That can be denoted as

$$\hat{r}_{ij} = Sigmoid(\sum \boldsymbol{\alpha} \odot \boldsymbol{\theta} - \beta), \boldsymbol{\theta} = \mathbf{h}_S, \beta = FC(\mathbf{h}_E), \boldsymbol{\alpha} = FC(\mathbf{h}_C), \quad (5)$$

where student ability feature  $\boldsymbol{\theta}$  and knowledge concept latent feature  $\boldsymbol{\alpha}$  are multidimensional and can handle multidimensional data [7]. Therefore, MIRT exhibits better performance than IRT without losing interpretability.

Different from the above traditional CDMs, MF [18] is originally devised for recommender systems but can be used for CD. MF holds very high interpretability because its prediction process [28] is very easy as  $\hat{r}_{ij} = \sum \mathbf{h}_S \odot \mathbf{h}_E$ . MF directly applies the inner product to student embedding  $\mathbf{h}_S$  and exercise embedding  $\mathbf{h}_E$  to compute the similarity. Larger similarity represents a higher probability of correctly the student answering the exercise. MF is quite simple yet effective compared to above CDMs.

## 2.2.2 Neural CDMs

To improve the diagnosis accuracy, Wang *et al.* tried to incorporate NNs with high-interpretability traditional CDMs like IRT and thus proposed a neural cognitive diagnosis framework (NCD) [28]. NCD's prediction is as

$$\begin{aligned} \mathbf{f}_S &= Sigmoid(\mathbf{h}_S), \mathbf{f}_{diff} = Sigmoid(\mathbf{h}_E), f_{disc} = Sigmoid(FC(\mathbf{h}_E)) \\ \hat{r}_{ij} &= FC_3(FC_2(FC_1(\mathbf{y}))), \mathbf{y} = \mathbf{h}_C \odot (\mathbf{f}_S - \mathbf{f}_{diff}) \times f_{disc} \end{aligned} \quad (6)$$

$\mathbf{f}_S \in \mathbb{R}^{1 \times K}$  represents student ability vector,  $\mathbf{f}_{diff} \in \mathbb{R}^{1 \times K}$  and  $f_{disc} \in \mathbb{R}^1$  represent exercise difficulty vector and distinction feature. The computation process of  $\mathbf{y}$  is similar to IRT, and  $\hat{r}_{ij}$  is obtained by applying three FC layers to  $\mathbf{y}$ . It can be seen the three-FC-layer is difficult to interpret in NCD. Although NCD attempts to utilize the monotonicity assumption to enhance its interpretability, the assumption can not make users understand how the diagnosis results are obtained. In summary, NCD indeed achieves promising improvements in diagnosis accuracy yet sacrifices its model interpretability to some extent.

As the follow-up work of NCD, KSCD [21] adjusts the positions of FC layers in NCD to obtain more meaningful student and exercise latent vectors by incorporating with knowledge concept vector first. Its prediction process can be denoted as

$$\begin{aligned} \hat{\mathbf{h}}_S &= Sigmoid(FC_1([\mathbf{h}_S, \mathbf{h}_C])), \hat{\mathbf{h}}_E = Sigmoid(FC_2([\mathbf{h}_E, \mathbf{h}_C])) \\ \hat{r}_{ij} &= (\sum \mathbf{h}_C \times (\hat{\mathbf{h}}_S - \hat{\mathbf{h}}_E))/D \end{aligned}, \quad (7)$$

where  $\hat{\mathbf{h}}_S$  and  $\hat{\mathbf{h}}_E$  are two latent vector with length of  $D$ . Despite the promising performance of KSCD, we can see the second equation can be interpreted yet the first one containing two FC layers holds poor interpretability.

As another representative of neural CDMs, the diagnostic function of RCD [13] gets the prediction  $\hat{r}_{ij}$  as follows:

$$\begin{aligned} \hat{\mathbf{h}}_S &= Sigmoid(FC_1([\mathbf{h}_S, \mathbf{h}_C])), \hat{\mathbf{h}}_E = Sigmoid(FC_2([\mathbf{h}_E, \mathbf{h}_C])) \\ \hat{r}_{ij} &= Sigmoid\left(\frac{1}{D} \sum FC_3(\hat{\mathbf{h}}_S - \hat{\mathbf{h}}_E)\right) \end{aligned} \quad (8)$$

Although previous papers [22] show RCD holds dominant performance over other neural CDMs, it can be seen that RCD's interpretability is worse than KSCD because the second equation further contains an FC layer.

### 2.3 Kolmogorov-Arnold Networks (KANs)

To address the lack of interpretability in existing neural CDMs, which can be mainly attribute to the opaque nature of the MLP. This paper aims to incorporate KANs into neural CDMs or directly leverage KANs for cognitive diagnosis because high model interpretability of KANs as shown in [19]. In the following, KANs will be introduced briefly.

A  $L$ -layer MLPs can be written as interleaving of transformations  $W$  and activations  $\sigma$ :

$$\text{MLP}(\mathbf{x}) = (W_{L-1} \circ \sigma \circ W_{L-2} \circ \sigma \circ \dots \circ W_1 \circ \sigma \circ W_0) \mathbf{x}, \quad (9)$$

which approximates complex functional mappings through multiple layers of nonlinear transformations. However, its deeply opaque nature constrains the model’s interpretability, posing challenges to intuitively understanding the internal decision-making process.

To address the issues of low parameter efficiency and poor interpretability in MLPs, Liu *et al.* [19] introduced the Kolmogorov-Arnold Network (KAN) that is inspired by Kolmogorov-Arnold representation theorem [17] [4]. Similar to MLP, a  $L$ -layer KAN can be described as a nesting of multiple KAN layers:

$$\text{KAN}(\mathbf{x}) = (\Phi_{L-1} \circ \Phi_{L-2} \circ \dots \circ \Phi_1 \circ \Phi_0) \mathbf{x}, \quad (10)$$

where  $\Phi_i$  represents the  $i$ -th layer of the whole KAN network. For each KAN layer with  $n_{in}$ -dimensional input and  $n_{out}$ -dimensional output,  $\Phi$  consist of  $n_{in} * n_{out}$  1-D learnable activation functions  $\phi$ :

$$\Phi = \{\phi_{q,p}\}, \quad p = 1, 2, \dots, n_{in}, \quad q = 1, 2, \dots, n_{out}. \quad (11)$$

When computing the result of the KAN network from layer  $l$  to layer  $l + 1$ , it can be represented in matrix form as follows:

$$\mathbf{x}_{l+1} = \underbrace{\begin{pmatrix} \phi_{l,1,1}(\cdot) & \phi_{l,1,2}(\cdot) & \dots & \phi_{l,1,n_l}(\cdot) \\ \phi_{l,2,1}(\cdot) & \phi_{l,2,2}(\cdot) & \dots & \phi_{l,2,n_l}(\cdot) \\ \vdots & \vdots & & \vdots \\ \phi_{l,n_{l+1},1}(\cdot) & \phi_{l,n_{l+1},2}(\cdot) & \dots & \phi_{l,n_{l+1},n_l}(\cdot) \end{pmatrix}}_{\Phi_l} \mathbf{x}_l. \quad (12)$$

In conclusion, KANs differentiate themselves from traditional MLPs by using learnable activation functions on the edges and parametrized activation functions as weights, eliminating the need for linear weight matrices. This design allows KANs to achieve comparable or superior performance with smaller model sizes. Moreover, their structure enhances model interpretability without compromising performance, making them suitable for applications like scientific discovery. In cognitive diagnostic tasks, KANs may offer precise diagnosis and analysis of learners’ knowledge structures, aiding personalized teaching and precision education with intuitive data interpretation.

## 3 The Proposed KA2NCD

**Overview.** Figure 2 presents the overview of the proposed KA2NCD containing two implementation manners. In the first manner (termed **KA2NCD-native**), all FC layers (MLPs) in the utilized CDM (NCD or KaNCD or KSCD or RCD) will be replaced by KANs with the same settings. In the second manner, there are two levels of KANs in the main module and two alternative embedding modules. In the main module, KANs at the lower level process the received student, exercise, and concept embeddings, while a KAN at the upper level combines and learns the lower KANs’ outputs to get the prediction. For the second manner, **KAN2CD-e** adopts the common embedding layers as its embedding module, while **KAN2CD-kan** adopts KANs as its embedding module.

### 3.1 Manner 1: KA2NCD-native

KA2NCD-native directly replaces all FC layers in the utilized neural CDM. For example, when adopting the NCD as the main module, KA2NCD-native (can be denoted as NCD+)

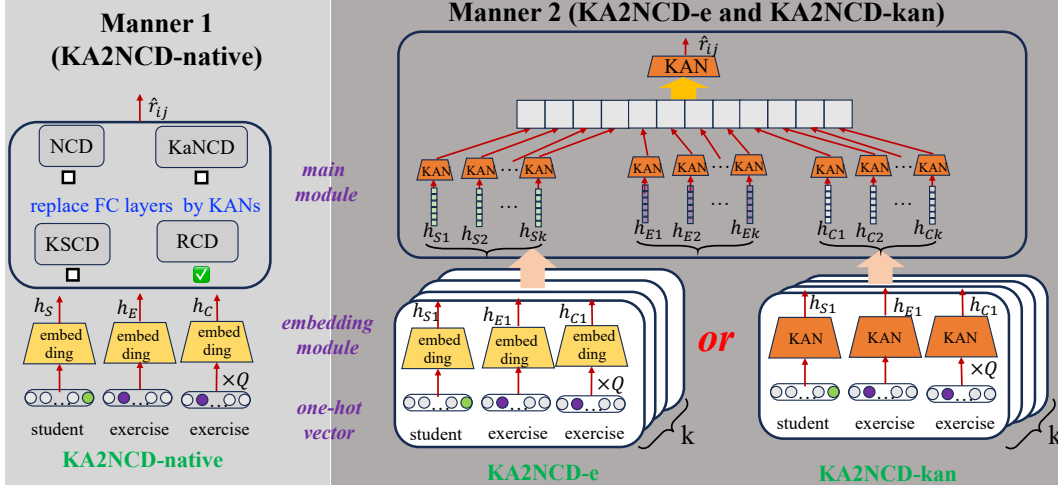


Figure 2: The Overview of the proposed KA2NCD, containing two implementation manners.

outputs the prediction  $\hat{r}_{ij}$  as

$$\begin{aligned} \mathbf{f}_S &= \text{Sigmoid}(\mathbf{h}_S), \mathbf{f}_{diff} = \text{Sigmoid}(\mathbf{h}_E), f_{disc} = \text{Sigmoid}(KAN_1(\mathbf{h}_E)) \\ \hat{r}_{ij} &= KAN_2(\mathbf{y}), \mathbf{y} = \mathbf{h}_C \odot (\mathbf{f}_S - \mathbf{f}_{diff}) \times f_{disc} \end{aligned} \quad (13)$$

$KAN_1(\cdot)$  is used to get the exercise difficulty scalar, and  $KAN_2(\cdot)$  is used to get  $\hat{r}_{ij}$  from  $\mathbf{y}$ . Due to the page limit, more KA2NCD-native variants (taking KaNCD, KSCD, and RCD as the main modules) can be found in **Appendix**, denoted as KaNCD+, KSCD+, and RCD+.

### 3.2 Manner 2: KA2NCD-e and KA2NCD-kan

Different from manner 1 under existing CDMs, in manner 2, a novel aggregation framework is designed for cognitive diagnosis based on KANs, which consists of two modules, i.e., the embedding module to get the input embedding and the main module to process input embedding and get the prediction.

#### 3.2.1 The embedding module

This paper designs two alternative embedding modules: the vanilla embedding module using the embedding layers and the KAN embedding module using KANs to get the embedding. For whichever type of embedding module, there are  $k$  sub-embedding modules to get  $k$  different initial embeddings  $\{\mathbf{h}_{S_i}, \mathbf{h}_{E_i}, \mathbf{h}_{C_i} | 1 \leq i \leq k\}$ . Multiple embeddings will provide diverse representations and may cause better learning results, which is similar to multiple heads in Transformer [27]

For the vanilla embedding module, each sub-embedding module's forward process is the same as Eq.(1), and the process of the vanilla embedding module can be denoted as

$$\begin{aligned} \mathbf{h}_{S_i} &= \mathbf{x}_i^S \times W_{S_i}, W_{S_i} \in \mathbb{R}^{N \times D}, \mathbf{h}_{E_i} = \mathbf{x}_i^E \times W_{E_i}, W_{E_i} \in \mathbb{R}^{M \times D} \\ \mathbf{h}_{C_i} &= \mathbf{x}_i^C \times W_{C_i}, W_{C_i} \in \mathbb{R}^{K \times D}, 1 \leq i \leq k. \end{aligned} \quad (14)$$

For the KAN embedding module, each sub-embedding module's forward process is as

$$\begin{aligned} \mathbf{h}_{S_i} &= KAN_{1*k}(\mathbf{x}_i^S | \Phi_{1*k}), \mathbf{h}_{E_i} = KAN_{2*k}(\mathbf{x}_i^E | \Phi_{2*k}), \Phi_2, \\ \mathbf{h}_{C_i} &= KAN_{3*k}(\mathbf{x}_i^C | \Phi_3), \Phi_3, \end{aligned}, 1 \leq i \leq k. \quad (15)$$

$\mathbf{h}_{S_i}$  has a length of  $D$ , and thus  $\Phi_{1*k}$  in  $KAN_{1*k}(\cdot)$  contains  $D \times N$  learnable functions to learn the embedding  $\mathbf{h}_{S_i}$ .  $\Phi_{2*k}$  and  $\Phi_{3*k}$  contains  $D \times M$  and  $D \times K$  learnable functions.

Table 1: Statistics of four popular education datasets.

Dataset	ASSISTments [12] ①	SLP [20] ②	JunYi [6] ③	FrcSub [1] ④
# Students/Concepts/Exercises	4,163/123/17,746	1,499/34/907	1000/39/712	536/8/20
# Response logs	324,572	57,244	203,945	10,720

### 3.2.2 The main module

After getting the input embedding set  $H = \{H_1, \dots, H_{3*k}\} = \{\mathbf{h}_{Si}, \mathbf{h}_{Ei}, \mathbf{h}_{Ci} | 1 \leq I \leq k\}$ , the main module is used to process these embeddings to get the final prediction  $\hat{r}_{ij}$  by two levels of KANs.

In the lower level, there are  $3 \times k$  KANs used for handling the input embedding set and obtaining the latent vector  $\mathbf{v} = \{v_1, v_2, \dots, v_{3*k}\}$ , where the forward pass is as follows:

$$v_i = KAN_i^{low}(H_i | \Phi_i^{low}), 1 \leq i \leq 3 * k. \quad (16)$$

Afterwards, in the upper level, a unified 2-layer KAN  $KAN^{up}$  is further used to process to the latent vector  $\mathbf{v}$  as

$$\hat{r}_{ij} = KAN^{up}(\mathbf{v} | \Phi_1^{up}, \Phi_2^{up}) = \Phi_2^{up} \circ \mathbf{ls} = \Phi_2^{up} \circ \Phi_1^{up} \circ \mathbf{v}, \quad (17)$$

where  $\Phi_1^{up}$  contains  $D \times 3 * k$  learnable functions and  $\Phi_2^{up}$  contains  $1 \times K$  learnable functions. Note that there is a latent vector  $\mathbf{ls} \in \mathbb{R}^{1 \times K}$  with length of  $K$ , which can be used to represent the student’s knowledge mastery vector.

While in manner 1, the student’s knowledge mastery vector (i.e., the student knowledge proficiency vector) is still represented by the latent student ability vector. For example,  $\mathbf{f}_S$  represents the student knowledge proficiency in NCD+ and KaNCD+, while  $\hat{\mathbf{h}}_S$  represents the student knowledge proficiency in KSCD+ and RCD+.

### 3.3 Model Training and Implementation Modification

**Model Training.** To train the proposed KA2NCD model, the Adam optimizer [16] is used to mine the following cross entropy loss [8] between model’s output  $\hat{r}_{ij}$  and true response  $r_{ij}$ :

$$\mathcal{L} = - \sum_{(s_i, e_j, r_{ij}) \in \mathcal{R}_{log}} (r_{ij} \log y_{ij}) + (1 - r_{ij}) \log (1 - y_{ij}). \quad (18)$$

**Implementation Modification.** The original implementation of KANs is not efficient because all intermediate variables  $X$  need to be expanded to perform different pre-given activation functions, which will require more memory and cost more to train. Considering most activation functions can be linear combinations [9] of a fixed set of B-splines basis functions  $B = \{B_1(\cdot), \dots, B_L(\cdot)\}$ , the process of one activation function can be rewritten as  $[B_1(X), \dots, B_L(X)] \times W_{linear}$ ,  $W_{linear} \in \mathbb{R}^{L \times 1}$ , i.e., activation with multiple basis functions and combine them linearly.

## 4 Experiments

The following experiments aim to answer the following researcher questions:

- **RQ1:** How about the effectiveness of manner 1 of KA2NCD?
- **RQ2:** How about the effectiveness of manner 2 of KA2NCD, i.e., KA2NCD-e(-kan)?
- **RQ3:** How about the interpretability (visualization) of KA2NCD?
- **RQ4:** How about the efficiency and complexity of the proposed KA2NCD?

### 4.1 Experimental Settings

**Datasets.** To verify the proposed KA2NCD, we conducted experiments on four real-world education datasets, including ASSISTments [12], SLP [20] JunYi [6] and FrcSub [1]. Their statistics are presented in Table 1, and more details can be found in **Appendix**.

Table 2: Performance comparison on four datasets. The best, second-best, and third-best results are in bold, underlined, and underwaved: KA2NCD-native’s results are not involved.

Dataset	Assistments		SLP		JunYi		FrcSub	
	AUC↑	ACC↑	AUC↑	ACC↑	AUC↑	ACC↑	AUC↑	ACC↑
Method								
IRT	72.02%	70.25%	80.91%	74.29%	74.80%	72.74%	80.63%	57.14%
MIRT	65.84%	63.90%	72.78%	71.90%	69.59%	69.50%	81.93%	69.12%
DINA	72.15%	68.06%	77.24%	71.43%	75.81%	68.18%	80.66%	83.12%
MF	70.55%	68.26%	79.22%	72.80%	79.48%	74.15%	84.10%	84.10%
NCD	74.84%	72.15%	84.76%	80.72%	80.70%	76.73%	90.12%	70.15%
NCD+	75.71%	71.91%	84.72%	80.38%	80.38%	76.12%	90.66%	74.30%
KaNCD	76.44%	<b>73.33%</b>	85.21%	81.61%	80.80%	76.15%	90.11%	76.68%
KaNCD+	76.99%	73.54%	85.25%	81.91%	82.06%	77.23%	91.44%	78.36%
RCD	75.91%	72.99%	85.57%	79.37%	<b>83.25%</b>	<b>78.67%</b>	89.39%	73.83%
RCD+	77.10%	73.78%	86.38%	80.12%	83.33%	78.76%	89.46%	74.53%
KSCD	76.55%	73.04%	85.90%	81.02%	82.17%	77.83%	90.49%	80.27%
KSCD+	76.72%	73.01%	86.06%	80.87%	<u>83.43%</u>	<u>78.67%</u>	90.66%	82.93%
KA2NCD-e	<b>76.64%</b>	72.96%	<b>86.08%</b>	<b>82.66%</b>	83.18%	78.39%	<b>91.27%</b>	<b>84.58%</b>
KA2NCD-kan	72.89%	<u>71.55%</u>	85.91%	81.91%	83.14%	78.41%	90.38%	83.30%

Table 3: Model parameter and training runtime comparisons between neural CDMs and KA2NCD on SLP & Junyi and ASSISTments & Junyi. (‘K’ means kilo, ‘h’ represents hours).

Param.	NCD	NCD+	KaNCD	KaNCD+	RCD	RCD+	KSCD	KSCD+	KA2NCD-kan	KA2NCD-e
SLP	232K	83K	91K	50K	279K	115K	94K	81K	4143K	471K
Junyi	219K	68K	79K	36K	266K	97K	74K	67401	3420K	416K
Runtime	NCD	NCD+	KaNCD	KaNCD+	RCD	RCD+	KSCD	KSCD+	KA2NCD-kan	KA2NCD-e
ASSIST	0.12h	0.17h	0.15h	0.2h	0.16h	0.28h	0.46h	1.12	15h	1.2h
JunYi	0.02h	0.02h	0.06h	0.08h	0.03h	0.03h	0.08h	0.13h	1.3h	0.33h

**Compared Models.** Four traditional CDMs (including IRT, MIRT, DINA, and MF) were taken as baselines. Besides, four neural CDMs (including NCD, KaNCD, KSCD, and RCD) are taken as baselines to validate the effectiveness of KA2NCD-native.

**Model Settings.** For all models, their embedding dimension  $D$  is set to the number of concepts  $K$ . The hyperparameters of comparison models follow the original papers. For KA2NCD, the batch size and learning rate are set to 128 and 0.002, the training epoch number is set to 20. All models were implemented in PyTorch and executed under an Intel 13700k CPU. Accuracy (ACC) and *Area Under the ROC Curve* (AUC) were used as evaluation metrics. **Our source code has been uploaded as a supplementary file.**

#### 4.2 Effectiveness of KA2NCD-native, KA2NCD-e, and KA2NCD-kan (RQ1 & RQ2)

To answer RQ1 and RQ2, Table 2 summarizes the performance of all compared CDMs on four datasets in terms of AUC and ACC values, and we can get the following observations.

Firstly, for KA2NCD-native variants, NCD+, KaNCD+, KSCD+, and RCD+ hold significantly better AUC and ACC performance than four traditional CDMs on three datasets (ASSISTments, SLP, and JunYi). On the FrcSub dataset, their AUC values are better than four traditional CDMs but their ACC values are worse than MF, whereas neural CDMs are also worse than MF regarding ACC values. Secondly, on ASSISTments and FrcSub datasets, KA2NCD-native variants hold better AUC values than NCD, KaNCD, KSCD, and RCD, where most of their ACC values are slightly better than neural CDMs. While for results on SLP and JunYi, most of KA2NCD-native variants’ results are similar to NCD, KaNCD, KSCD, and RCD, but some of their results are still superior (such as RCD+ on both datasets, KaNCD+ on JunYi, and KSCD+ on Junyi). Thirdly, compared to existing CDMs, KA2NCD-e nearly achieves the top-best performance on all datasets, while KA2NCD-kan’s performance is worse than KA2NCD-e and not very promising, especially on ASSISTments. However, the performance of KA2NCD-kan on the other three datasets is still promising, which is slightly worse than KSCD but better than other CDMs.

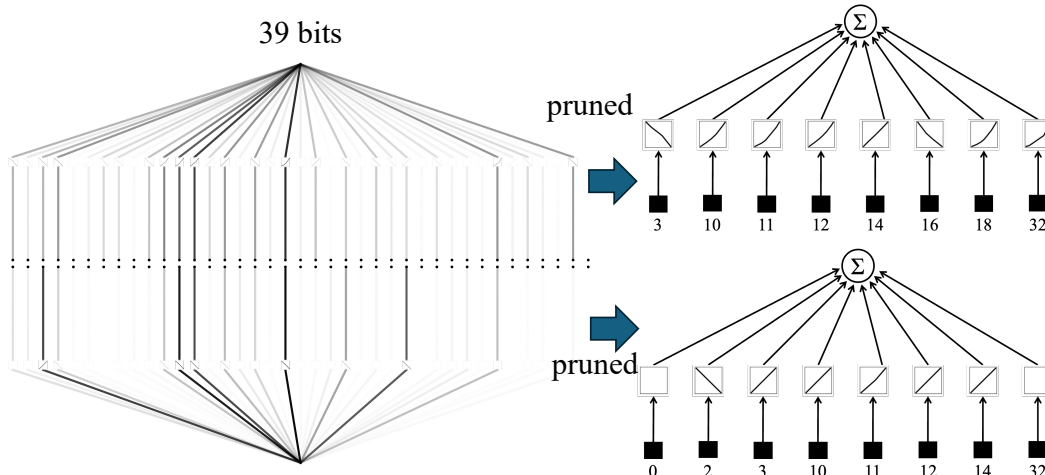


Figure 3: Visualization of NCD+ (upper) and KaNCD+ (lower) on JunYi datasets.

The first two observations show the proposed KA2NCD in manner 1 (i.e., KA2NCD-native) is effective. The third one demonstrates the superiority of KA2NCD-e and KA2NCD-kan’s effectiveness, further indicating leveraging KANs for CD is promising and worth exploring.

### 4.3 Visualization of KA2NCD (RQ3)

To answer RQ3, Figure 3 plots the structures of NCD+ and KaNCD+ only on the JunYi dataset because its  $K$  is relatively small. The structure visualization of NCD+ and KaNCD+ on SLP can be found in **Appendix**. In Figure 3, only the last KAN in NCD+ and KaNCD+ is plotted because they replace MLPs to get the prediction. As can be seen, firstly, the learned structures of their KANs are very close, which indicates the learned KAN has good transferability between two models; secondly, only about 8 of 39 connections are kept in both models, which represents the learned models are easy to interpret how they work. Similar observations and conclusions can be drawn from the Figures in **Appendix**, which shows the proposed KA2NCD can indeed enhance the interpretability of existing CDMs.

### 4.4 Complexity and Efficiency of KA2NCD (RQ4)

To show the model complexity of the proposed KA2NCD, Table 3 presents the comparison of neural CDMs, KA2NCD-native variants, KA2NCD-e, and KA2NCD-kan regarding model parameter number and runtime of training models. As can be seen, the parameters of KA2NCD-native are less than half of the corresponding neural CDM, while parameters of KA2NCD-e and KA2NCD-kan are much more than neural CDMs, especially for KA2NCD-kan. The high parameters of KA2NCD-kan lead to its extremely high runtime. Despite that, the runtimes of KA2NCD-native are close to those of neural CDMs, which indicates the efficiency of KA2NCD is competitive and acceptable. The good efficiency is attributed to our modified implementations of KANs, because the original implementation of KANs is very slow: on ASSISTments and JunYi, NCD+ took about 0.9 and 0.3 hours, and KaNCD+ took about 1.1 and 0.35 hours, which is four times as our modified KANs.

## 5 Conclusion

In this paper, we proposed to enhance the model interpretability of neural CDMs by leveraging KANs, and thus we proposed KA2NCD. There are two manners to implement KA2NCD, where the first manner directly replaces MLPs in existing neural CDM by KANs and the second manner builds a novel CDM completely with KANs. Experimental results demonstrate the effectiveness of the proposed KA2NCD and its high interpretability.

## References

- [1] AICFE. Frctest dataset. <http://staff.ustc.edu.cn/%7Eqiliuql/data/math2015.rar>, 2018.
- [2] Ashton Anderson, Daniel Huttenlocher, Jon Kleinberg, and Jure Leskovec. Engaging with massive online courses. In *Proceedings of the 23rd International Conference on World Wide Web*, pages 687–698, 2014.
- [3] Joseph Beck. Difficulties in inferring student knowledge from observations (and why you should care). In *Proceedings of the 13rd International Conference of Artificial Intelligence in Education*, pages 21–30, 2007.
- [4] Jürgen Braun and Michael Griebel. On a constructive proof of kolmogorov’s superposition theorem. *Constructive approximation*, 30:653–675, 2009.
- [5] Hugh Burns, Carol A Luckhardt, James W Parlett, and Carol L Redfield. *Intelligent Tutoring Systems: Evolutions in design*. Psychology Press, 2014.
- [6] Haw-Shiuan Chang, Hwai-Jung Hsu, Kuan-Ta Chen, et al. Modeling exercise relationships in e-learning: A unified approach. In *Proceedings of the 2015 International Educational Data Mining Society (EDM)*, pages 532–535, 2015.
- [7] Song Cheng, Qi Liu, Enhong Chen, Zai Huang, Zhenya Huang, Yiyang Chen, Haiping Ma, and Guoping Hu. Dirt: Deep learning enhanced item response theory for cognitive diagnosis. In *Proceedings of the 28th ACM International Conference on Information and Knowledge Management*, pages 2397–2400, 2019.
- [8] Pieter-Tjerk De Boer, Dirk P Kroese, Shie Mannor, and Reuven Y Rubinstein. A tutorial on the cross-entropy method. *Annals of operations research*, 134:19–67, 2005.
- [9] Carl De Boor and Carl De Boor. *A practical guide to splines*, volume 27. springer-verlag New York, 1978.
- [10] Susan E Embretson and Steven P Reise. *Item Response Theory*. Psychology Press, 2013.
- [11] Feng-Lei Fan, Jinjun Xiong, Mengzhou Li, and Ge Wang. On interpretability of artificial neural networks: A survey. *IEEE Transactions on Radiation and Plasma Medical Sciences*, 5(6):741–760, 2021.
- [12] Mingyu Feng, Neil Heffernan, and Kenneth Koedinger. Addressing the assessment challenge with an online system that tutors as it assesses. *User Modeling and User-adapted Interaction*, 19(3):243–266, 2009.
- [13] Weibo Gao, Qi Liu, Zhenya Huang, Yu Yin, Haoyang Bi, Mu-Chun Wang, Jianhui Ma, Shijin Wang, and Yu Su. Rcd: Relation map driven cognitive diagnosis for intelligent education systems. In *Proceedings of the 44th International ACM SIGIR Conference on Research and Development in Information Retrieval*, pages 501–510, 2021.
- [14] Liya Hu, Zhiang Dong, Jingyuan Chen, Guifeng Wang, Zhihua Wang, Zhou Zhao, and Fei Wu. Ptadisc: A cross-course dataset supporting personalized learning in cold-start scenarios. In *Proceedings of the 37th Conference on Neural Information Processing Systems Datasets and Benchmarks Track*, 2023.
- [15] Eric Jang, Shixiang Gu, and Ben Poole. Categorical reparameterization with gumbel-softmax. *arXiv preprint arXiv:1611.01144*, 2016.
- [16] Diederik P Kingma and Jimmy Ba. Adam: A method for stochastic optimization. *arXiv preprint arXiv:1412.6980*, 2014.
- [17] Andreï Kolmogorov. *On the representation of continuous functions of several variables by superpositions of continuous functions of a smaller number of variables*.
- [18] Yehuda Koren, Robert Bell, and Chris Volinsky. Matrix factorization techniques for recommender systems. *Computer*, 42(8):30–37, 2009.

- [19] Ziming Liu, Yixuan Wang, Sachin Vaidya, Fabian Ruehle, James Halverson, Marin Soljačić, Thomas Y Hou, and Max Tegmark. Kan: Kolmogorov-arnold networks. *arXiv preprint arXiv:2404.19756*, 2024.
- [20] Yu Lu, Yang Pian, Ziding Shen, Penghe Chen, and Xiaoqing Li. SLP: A multi-dimensional and consecutive dataset from K-12 education. In *Proceedings of the 29th International Conference on Computers in Education Conference*, volume 1, pages 261–266, 2021.
- [21] Haiping Ma, Manwei Li, Le Wu, Haifeng Zhang, Yunbo Cao, Xingyi Zhang, and Xuemin Zhao. Knowledge-sensed cognitive diagnosis for intelligent education platforms. In *Proceedings of the 31st ACM International Conference on Information & Knowledge Management*, pages 1451–1460, 2022.
- [22] Haiping Ma, Jinwei Zhu, Shangshang Yang, Qi Liu, Haifeng Zhang, Xingyi Zhang, Yunbo Cao, and Xuemin Zhao. A prerequisite attention model for knowledge proficiency diagnosis of students. In *Proceedings of the 31st ACM International Conference on Information & Knowledge Management*, pages 4304–4308, 2022.
- [23] Thanaporn Patikorn, Neil T Heffernan, and Ryan S Baker. Assistments longitudinal data mining competition 2017: A preface. In *Proceedings of the 2018 International Conference on Educational Data Mining*, 2018.
- [24] Mark D Reckase. *Multidimensional Item Response Theory Models*. Springer, 2009.
- [25] Wojciech Samek, Alexander Binder, Grégoire Montavon, Sebastian Lapuschkin, and Klaus-Robert Müller. Evaluating the visualization of what a deep neural network has learned. *IEEE Transactions on Neural Networks and Learning Systems*, 28(11):2660–2673, 2016.
- [26] D. L. Torre and J. Dina model and parameter estimation: A didactic. *Journal of Educational and Behavioral Statistics*, 34(1):115–130, 2009.
- [27] Ashish Vaswani, Noam Shazeer, Niki Parmar, Jakob Uszkoreit, Llion Jones, Aidan N Gomez, Łukasz Kaiser, and Illia Polosukhin. Attention is all you need. *Advances in neural information processing systems*, 30, 2017.
- [28] Fei Wang, Qi Liu, Enhong Chen, Zhenya Huang, Yuying Chen, Yu Yin, Zai Huang, and Shijin Wang. Neural cognitive diagnosis for intelligent education systems. In *Proceedings of the 2020 AAAI Conference on Artificial Intelligence*, volume 34, pages 6153–6161, 2020.
- [29] Fei Wang, Qi Liu, Enhong Chen, Zhenya Huang, Yu Yin, Shijin Wang, and Yu Su. Neuralcd: a general framework for cognitive diagnosis. *IEEE Transactions on Knowledge and Data Engineering*, 2022.
- [30] Shangshang Yang, Haoyu Wei, Haiping Ma, Ye Tian, Xingyi Zhang, Yunbo Cao, and Yaochu Jin. Cognitive diagnosis-based personalized exercise group assembly via a multi-objective evolutionary algorithm. *IEEE Transactions on Emerging Topics in Computational Intelligence*, 7(3):829–844, 2023.
- [31] Yu Zhang, Peter Tiño, Aleš Leonardis, and Ke Tang. A survey on neural network interpretability. *IEEE Transactions on Emerging Topics in Computational Intelligence*, 5(5):726–742, 2021.

## A More Details

### A.1 KA2NCD-native Variants

**KSCD+**. When adopting the KSCD as the main module, the prediction process of KA2NCD-native (further denoted as KSCD+) is as

$$\begin{aligned} \hat{\mathbf{h}}_S &= \text{Sigmoid}(KAN_1([\mathbf{h}_S, \mathbf{h}_C])), \hat{\mathbf{h}}_E = \text{Sigmoid}(KAN_2([\mathbf{h}_E, \mathbf{h}_C])) \\ \hat{r}_{ij} &= \left( \sum \mathbf{h}_C \times (\hat{\mathbf{h}}_S - \hat{\mathbf{h}}_E) \right) / D \end{aligned}, \quad (19)$$

where the first KAN  $KAN_1(\cdot)$  is used to combine student embedding and concept embedding to get the richer student ability vector and the second KAN  $KAN_2(\cdot)$  is used to get the richer exercise difficulty vector.

**RCD+**. When adopting the RCD as the main module, the prediction of KA2NCD-native (further denoted as RCD+) can be obtained according to the following process:

$$\begin{aligned} \hat{\mathbf{h}}_S &= \text{Sigmoid}(KAN_1([\mathbf{h}_S, \mathbf{h}_C])), \hat{\mathbf{h}}_E = \text{Sigmoid}(KAN_2([\mathbf{h}_E, \mathbf{h}_C])) \\ \hat{r}_{ij} &= \text{Sigmoid}\left(\frac{1}{D} \sum KAN_3(\hat{\mathbf{h}}_S - \hat{\mathbf{h}}_E)\right) \end{aligned}. \quad (20)$$

where the first two KANs are the same as those of KSCD+, which is used to get a richer student ability vector and a richer exercise difficulty vector. The third KAN  $KAN_3(\cdot)$  is used to extract the response prediction.

**KaNCD+**. When adopting the KaNCD as the main module, we can follow the following equation to get the prediction of KA2NCD-native (further denoted as KaNCD+):

$$\begin{aligned} \mathbf{f}_S &= \text{Sigmoid}(KAN_1(\mathbf{h}_S)), \mathbf{f}_{diff} = \text{Sigmoid}(KAN_2(\mathbf{h}_E)), \mathbf{f}_{disc} = \text{Sigmoid}(KAN_3(\mathbf{h}_E)) \\ \hat{r}_{ij} &= KAN_4(\mathbf{y}), \mathbf{y} = \mathbf{h}_C \odot (\mathbf{f}_S - \mathbf{f}_{diff}) \times \mathbf{f}_{disc} \end{aligned}. \quad (21)$$

It can be seen that the last two KANs have the same effect as that of NCD+, and the first and second KANs are used to get the enhanced student ability vector and exercise difficulty vector.

### A.2 Details about datasets

The detailed descriptions of four datasets are as follows:

- **ASSISTments** [12] is an openly available dataset created in 2009 by the ASSISTments online tutoring service system. Here we adopted the public corrected version that does not contain duplicate data. The dataset contains more than 4,000 students, nearly 18,500 exercises, and over 300,000 response logs.
- **SLP** [20] is another public education dataset published in 2021. SLP collects learners' regularly captured academic performance data during their three-year studies in eight subjects: Chinese, mathematics, English, physics, chemistry, biology, history, and geography.
- **JunYi** [6] JunYi is a public dataset collected by the JunYi Education Platform in Taiwan, containing nearly 20M responses from 1,000 students. E-Math is a private dataset collected by a well-known electronic educational product, mainly containing primary and secondary school students' math exercises and test logs.
- **FrcSub**<sup>1</sup> The FrcSub dataset, commonly utilized for evaluating cognitive diagnosis models, focuses on fraction addition and subtraction problems. It encompasses performance data from 536 learners across 20 objective questions, with scores represented as binary values (1 for correct, 0 for incorrect). Additionally, it includes a knowledge point correlation matrix that details the relationship between the 20 questions and 8 distinct knowledge points, where a value of 1 indicates a related knowledge point, and 0 indicates no relation. This dataset serves as a valuable resource for cognitive modeling research.

For the four datasets, we filtered out students with fewer than 15 response logs to ensure sufficient data for model learning. Each student's logs are randomly split into training and testing datasets at the splitting ratio of 7/3.

<sup>1</sup><http://staff.ustc.edu.cn/%7Eqiliuql/data/math2015.rar>

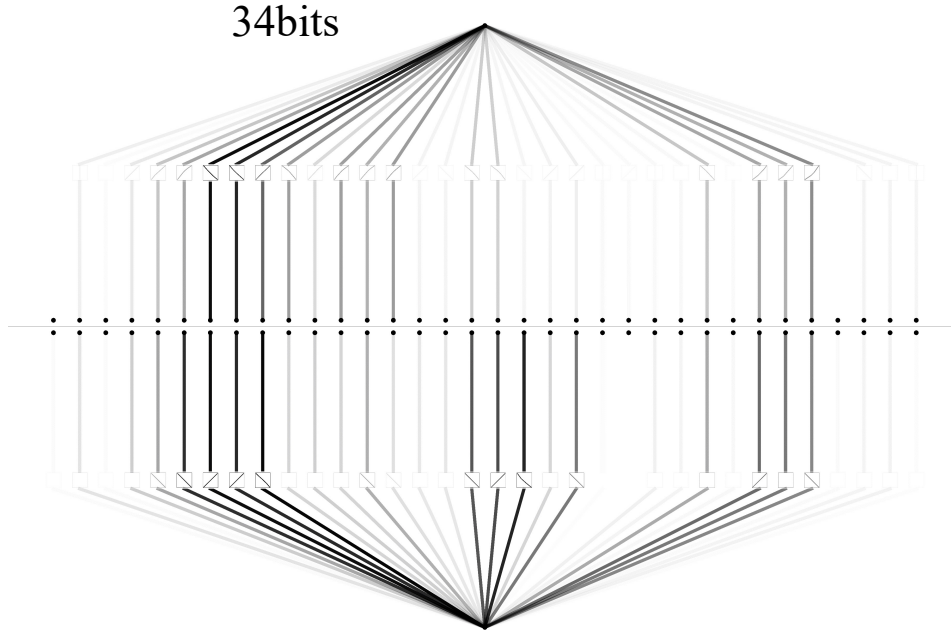


Figure 4: Overview-Visualization of KANs in NCD+ (upper) and KaNCD+ (lower) on the SLP datasets.

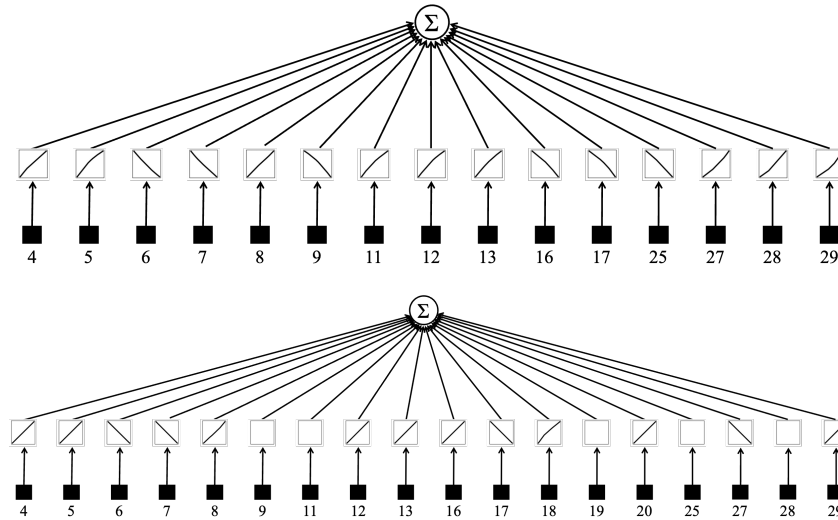


Figure 5: Visualization of pruned KANs in NCD+ (upper) and KaNCD+ (lower) on the SLP datasets.

## B More Visualization

For deep insight into the learned KANs' structures to answer **RQ3**, Figures 4 and 5 plot the structures of NCD+ and KaNCD+ learned on the SLP dataset, Figure 6 plots the structures of KA2NCD-e learned on the JunYi dataset, while Figure 7 plots the structures of KA2NCD-e learned on the SLP dataset. For easy observation, for Figure 4, only the last KAN in NCD+ and KaNCD+ is plotted because they replace MLPs to get the prediction; while for Figures 6 and 7, only the structures of the upper-level KANs are presented.

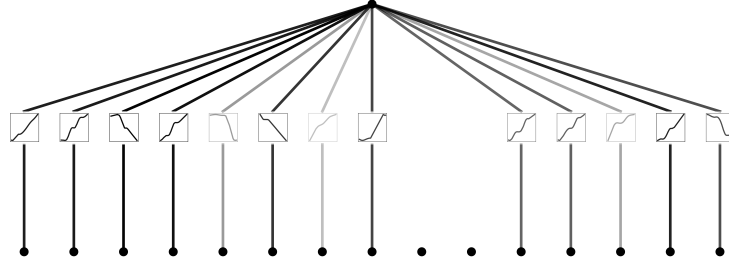


Figure 6: Visualization of the last KAN in KA2NCD-e ) on the JunYi datasets.

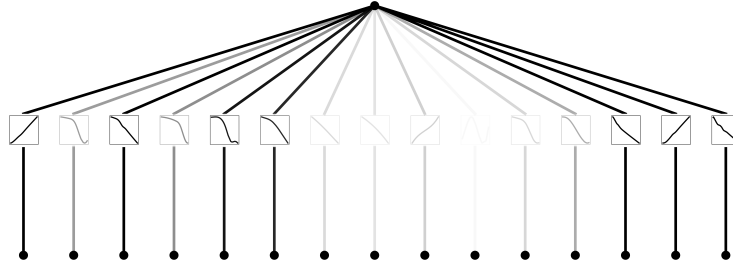


Figure 7: Visualization of KA2NCD-e (upper) on the SLP datasets.

As can be seen from Figures 4 and 5, the learned structures of KANs are very close, which indicates the learned KAN has good transferability between two models; about 15 of 34 connections are kept in both models, which makes the learned models easy to be interpreted. As can be seen from Figures 6 and 7, which latent features are used and how they are combined can be obviously observed, which is very important for users to understand.

In conclusion, the proposed KA2NCD can indeed enhance the interpretability of existing CDMs, and the manner 2 of the proposed KA2NCD is indeed effective, where the learned structures are really easy to interpret.